RESEARCH ARTICLE

Editorial Process: Submission:12/16/2025 Acceptance:07/18/2026 Published:07/27/2026

Agarose-Based 3D Spheroid Model to Evaluate the Anticancer Activity of the Curcumin Analog CCA-1.1 in Triple-Negative Breast Cancer

Ika Rahmawati Sutejo[1,2,3], Riris Istighfari Jenie[1,4]*, Muthi Ikawati[1,4,5], Sofia Mubarika Haryana[5,6], Ikhlas Muhammad Jenie[7], Chio Oka[8]

Abstract

Background: Three-dimensional (3D) cell culture systems provide superior simulation of the tumour microenvironment compared to traditional two-dimensional (2D) cultures. Chemoprevention agent curcumin analog-1.1 (CCA-1.1), a synthetic curcumin derivative, has demonstrated promising anticancer properties against triple-negative breast cancer (TNBC). This study aimed to develop and use a 3D agarose-based culture system for MDA-MB-231 cells to comprehensively evaluate the efficacy of CCA-1.1 as an anticancer agent. **Methods:** MDA-MB-231 breast cancer cells were cultured in both a 2D monolayer and a 3D agarose-based spheroid system. Cytotoxicity was assessed using CCK-8 assays, and IC_{50} values were determined. Spheroid formation capacity was evaluated and compared with that of doxorubicin. Propidium iodide staining was performed to assess cell viability and structural integrity. Gene expression analysis of epithelial-mesenchymal transition (EMT) markers and metastasis-related proteins (*E-cadherin*, *MMP2*, and *MMP9*) was conducted using qRT-PCR. **Results:** CCA-1.1 demonstrated IC_{50} values of 1.48±0.28 μM in 2D cultures versus 6.12±0.27 μM in 3D cultures, while doxorubicin showed IC_{50} values of 0.79±0.22 μM (2D) and 2.65±0.3 μM (3D). CCA-1.1 reduced spheroid formation by 40% compared to controls, whereas doxorubicin achieved 96% inhibition. Propidium iodide staining showed that CCA-1.1 induced cell death while preserving the spheroid structure, unlike doxorubicin, which disrupted the architecture. Expression level analysis revealed that CCA-1.1 reduced *MMP2* (0.15-fold, p=0.0001) and *MMP9* (0.25-fold, p<0.0001) levels while increasing *E-cadherin* levels by 1.54-fold (p=0.379). **Conclusion:** Our study using a 3D agarose-based spheroid culture confirms the cytotoxicity of CCA-1.1 against MDA-MB-231 and showed that the compound inhibited spheroid formation and epithelial-mesenchymal transition, and reduced the expression levels of matrix metalloproteinases. These data support the development of CCA-1.1 as a candidate chemotherapeutic agent for TNBC.

Keywords: 3D cell culture- EMT- MDA-MB-231- metastasis- matrix metalloproteinase

Asian Pac J Cancer Prev, **27 (7)**, 2689-2696

Introduction

Triple-negative breast cancer (TNBC) is a subtype of breast cancer with the absence of estrogen receptor (ER), progesterone receptor (PR), and human epidermal growth factor receptor 2 (HER2) expression, which presents high invasiveness and poor prognosis [1, 2]. Such a lack largely restricts available therapies and thus implies a dismal prognosis of TNBC, with higher mortality than other molecular subtypes [2, 3]. TNBC accounts for about 15–20% of breast cancer worldwide, and tends to be diagnosed in younger women. Its aggressive behavior results in metastasis at an early stage with substantial clinical and socio-economic implications [4]. Despite chemotherapy continuing to be a mainstay approach in treatment practice, it is clouded by matters like drug resistance and severe side effects that hinder the long-term effectiveness of therapies [3, 5]. This highlights the pressing need to develop new therapeutic drugs with greater efficacy and lower toxicity to improve patient survival outcomes [2, 6].

To address this therapeutic problem, curcumin and

*[1]Cancer Chemoprevention Research Center, Faculty of Pharmacy, Universitas Gadjah Mada, Yogyakarta 55281, Indonesia. [2]Department of Biochemistry, Faculty of Medicine, Universitas Jember, Jember 68121, Indonesia. [3]Biotechnology Doctorate Study Program, Graduate School, Universitas Gadjah Mada, Yogyakarta 55281, Indonesia. [4]Laboratory of Macromolecular Engineering, Department of Pharmaceutical Chemistry, Faculty of Pharmacy, Universitas Gadjah Mada, Yogyakarta 55281, Indonesia. [5]Study Center for Biotechnology, Universitas Gadjah Mada, Yogyakarta 55281, Indonesia. [6]Faculty of Medicine, Nursing, and Public Health, Universitas Gadjah Mada, Yogyakarta 55281, Indonesia. [7]Faculty of Medicine and Health Sciences, Universitas Muhammadiyah Yogyakarta, Yogyakarta 55183, Indonesia. [8]Functional Genomics and Medicine, Division of Biological Sciences, Nara Institute of Science and Technology, Nara, 6300101, Japan. *For Correspondence: riris_jenie@ugm.ac.id Ad magnia cum*

its derivatives have been shown to possess potential anticancer effects in different types of cancers [7]. Chemoprevention Curcumin Analog-1.1 (CCA-1.1), a curcumin structural analog, has shown significant anticancer effects in laboratory studies against various cancer cells, including breast cancer, colon cancer, chronic myeloid leukemia, and hepatocellular cancer cells [8-12]. These compounds exert multiple mechanisms, including cell cycle arrest, induction of apoptosis, and suppression of cancer cell migration and invasion, which are highly attractive for TNBC therapy [8]. Expanding on its potential, CCA-1.1 has demonstrated antimigratory activity and the ability to sensitize tumor cells to cytostatic drugs through synergistic mechanisms, suggesting it may serve as a co-therapeutic agent.

Despite these strides in agent discovery, conventional in vitro assessments in two-dimensional (2D) cell culture settings often poorly simulate the three-dimensional tumor niche and lead to the exaggeration of drug activity by virtue of lacking interactions with the extracellular matrix and tissue architecture [13]. On the other hand, 3D culture more closely reflects in vivo conditions, such as nutrient gradients and cell-to-cell interactions, thereby eliciting more physiologically relevant drug responses [5, 14]. MDA-MB-231 cells, a commonly used TNBC cell line, are also more resistant to drugs in 3D than in 2D cultures, underscoring the need of test novel compounds in both culture systems to improve clinical relevance [15, 16]. In addition, the evaluation of other phenotypic endpoints, including spheroid-forming ability, cell death mechanisms, expression of epithelial-mesenchymal transition (EMT), and metastasis-associated genes within the 3D model systems, offers a more thorough mechanistic understanding of drug response, going beyond mere assessment of cytotoxicity.

Therefore, in this study, we aimed to develop an agarose-based spheroid of MDA-MB-231 cells to assess and compare the cytotoxicity of CCA-1.1 and to evaluate its effectiveness relative to doxorubicin, a control anthracycline-based chemotherapy drug, in 2D monolayer and 3D spheroidal models. We would therefore expect that 3D cultures would exhibit a higher IC_{50} value, consistent with the drug-resistant tumour microenvironment, and that CCA-1.1 could exhibit potential multi-targeted anticancer activity (inhibition of cancer stem cell populations, induction of apoptosis, regulation of EMT markers, and inhibition of EMT-associated genes) that could be developed into a therapeutic agent for TNBC.

Materials and Methods

Cell Culture and Compounds

The MDA-MB-231 triple-negative breast cancer cell line (ATCC HTB-26) was from the Functional Genomics and Medicine Laboratory, Division of Biological Science, Nara Institute of Science and Technology, Ikoma, Nara, Japan. The MDA-MB-231 cell line was studied in both 2D and 3D culture. The cells for 2D monolayer models were kept in Dulbecco's Modified Eagle Medium (DMEM; Gibco, Thermo Fisher Scientific, USA) containing 10% foetal bovine serum (FBS; Gibco, USA), and incubated at 37°C in a humidified 5% CO_2 atmosphere. For 3D models, the same DMEM was supplemented with 10% FBS, 1 μg/mL hydrocortisone, 20 ng/mL epidermal growth factor (EGF), and 2 ng/mL transforming growth factor-β1 (TGF-β1), all from Sigma-Aldrich (USA). Doxorubicin (FUJIFILM Wako, Japan) was used as the reference drug for cytotoxicity in triple-negative breast cancer. CCA-1.1, synthesized at CCRC, UGM, Indonesia, and characterized as described previously [10], was used as an experimental compound and dissolved in dimethyl sulfoxide (DMSO; Merck KGaA, Germany). The final concentration of DMSO in cell cultures was ≤0.5% (v/v).

Cytotoxicity and Proliferative Assay

Cell viability and cytotoxicity were assessed using the Cell Counting Kit-8 (CCK-8; Dojindo Molecular Technologies, Japan) according to established protocols. For 2D models, 5×10^3 cells per well were seeded in 96-well plates, incubated for 24 hours, and then treated with serial concentrations of doxorubicin and CCA-1.1 (0.125–8 μM), followed by the addition of CCK-8 reagent and a 2-hour incubation before absorbance was measured at 450 nm to assess cell viability. For 3D models, spheroids were generated by seeding cells in 1.5% (w/v) agarose-coated 96-well plates and allowing spheroid formation over 72 hours. Spheroids were treated with CCA-1.1 (1–30 μM) for 96 hours. Post-treatment, cell viability was quantified using the CCK-8 assay, and absorbance was read at 450 nm. Spheroid morphology was monitored daily using an inverted microscope.

Spheroid Forming Assay

MDA-MB-231 cells were treated with CCA-1.1 at the IC_{50} concentration (6 μM) before being resuspended in medium (DMEM/F12 supplemented with 2 mM L-glutamine, 20 ng/mL EGF, 10 ng/mL bFGF) (Gibco/Sigma-Aldrich, USA). A total of 5×10^4 cells per well were seeded onto 24-well agarose-coated plates using 500 μL of medium per well, and the plates were incubated for 7 days at 37°C in 5% CO2. Daily observations were recorded at 10× magnification using an inverted microscope. Spheroid diameter and area were analyzed using ImageJ (NIH, USA) with a minimum size threshold of 300 μm. The spheroid diameter of 300 μm or larger is anticipated to be composed of three concentric layers, which represent the proliferating, quiescent, and necrotic cores [17]. Spheroid-forming potential was expressed as the number of spheroids per 50,000 cells (±SE) from three independent replicates.

Propidium Iodide Staining for Evaluation of Spheroid Response

We conducted the experiment to evaluate spheroid response using propidium iodide (PI) staining, as described by Brüningk et al. [18]. The MDA-MB-231 cells (1×10^4 per well) were seeded onto 96-well agarose-coated plates and cultured for 3 days to form spheroids. Spheroids were treated with CCA-1.1 at the IC_{50} concentration (6 μM) for 24 hours. Post-treatment spheroids were stained with propidium iodide (PI; Sigma-Aldrich, USA) at 5 μg/mL in serum-free DMEM/F12 medium for 10 minutes at room

temperature in the dark. After PBS washing, spheroids were transferred to glass-bottomed imaging plates and examined using confocal microscopy (LSM 900; Zeiss, Germany) with a 40× objective. PI fluorescence (excitation 535 nm, emission 617 nm) was detected via z-stack imaging at 10 µm intervals to visualize dead cells.

qRT-PCR

Total RNA from CCA-1.1-treated 3D spheroids at the IC_{50} for 24 hours was extracted using the Total RNA Mini Kit (Favogen Biotech, Taiwan) according to the manufacturer's instructions. After gDNA Eraser treatment, 1 µg RNA was reverse transcribed using PrimeScript RT Reagent Kit (Takara Bio, Japan). cDNA samples were amplified in triplicate using SYBR Premix Ex Taq II and LightCycler 96 PCR System (Roche, Swiss) with the following conditions: 95°C for 1 minute; 45 cycles at 95°C for 10 seconds, 55°C for 30 seconds, and 72°C for 20 seconds; followed by dissociation curve analysis. Dissociation curves confirmed specific target amplification. Gene expression data were analyzed using the ΔΔCt method with GAPDH as an internal control. Fold-changes were expressed as mean ± SE from three replicates. Primer sequences for EMT markers and GAPDH are listed in Table 1.

Data Analysis

IC_{50} values were determined by nonlinear regression using Microsoft Excel, based on at least three independent replicates per condition. Statistical analysis of the Spheroid Forming Assay was performed using GraphPad Prism (version 9.0; GraphPad Software, USA) with unpaired t-tests ($p<0.05$). Results are expressed as mean±standard deviation (SD). Statistical comparisons between 2D and 3D conditions were made using unpaired t-tests, and significance was set at $p<0.05$.

Results

Spheroid formation in 3D agarose culture

MDA-MB-231 cells seeded on 1.5% (w/v) agarose produced compact, uniformly spherical aggregates within 72 h. Mean spheroid diameter increased, and after which size plateaued. No spontaneous disintegration or necrotic core formation was observed during the 96 h treatment window, confirming model stability for drug-response analyses.

Cytotoxicity in 2D monolayer and agarose-based 3D spheroid cultures

Dose-response curves generated with the CCK-8 assay revealed sub-micromolar potency for all compounds. Doxorubicin produced the IC_{50} (0.79 ± 0.22 µM) and CCA-1.1 (1.48 ± 0.28 µM). Cell morphology after 48 h displayed typical apoptotic features cell rounding, shrinkage, and detachment (Figure 1).

Cytotoxicity was markedly reduced in 3D spheroids.

Table 1. Primer Sequences for qRT-PCR Analysis of Metastasis & EMT-Related Genes

No	Gene	Primer
1	*Vimentin*	Forward: 5'- AGATGGCCCTTGACATTGAG-3'
		Reverse: 5'- TGGAAGAGGCAGAGAAATCC-3'
2	*E-cadherin (CDH1)*	Forward: 5'- CGAGAGCTACACGTTCACGG-3'
		Reverse: 5'- GGGTGTCGAGGGAAAAATAGG-3'
3	*N-cadherin (CDH2)*	Forward: 5′-AATCAGTGGCGGAGATCCTAC-3′
		Reverse: 5′-TTGACCACGGTGACTAACCC-3′
4	*MMP9*	Forward: 5′-TTCCAGTACCGAGAGAAAGCCTAT-3′
		Reverse: 5′-GGTCACGTAGCCCACTTGGT-3′
5	*MMP2*	Forward: 5'-TACAGGATCATTGGCTACACACC-3'
		Reverse: 5'-GGTCACATCGCTCCAGACT-3'
6	*GAPDH*	Forward: 5′-GACAGTCAGCCGCATCTTCT-3′
		Reverse: 5′-TTAAAAGCAGCCCTGGTGAC-3′

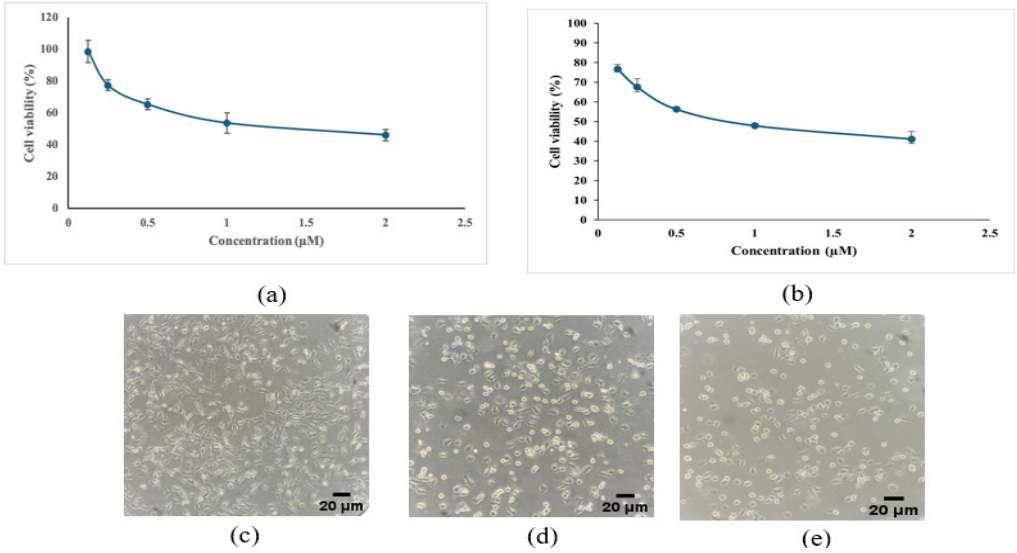

Figure 1. Cytotoxicity of CCA-1.1 and Doxorubicin (Dox) in MDA-MB-231 2D Monolayer Cultures. MDA-MB-231 cells were seeded as detailed in the Methods, and the cytotoxicity of (a) CCA-1.1 and (b) Dox was assessed using CCK-8. Data represent mean ± SD from three independent experiments. The cell morphology of (c) the untreated group, (d) the CCA-1.1-treated group, and (e) the doxorubicin-treated group under an inverted microscope (total magnification 100×).

Table 2. Comparison of the Cytotoxicity of CCA-1.1 and Doxorubicin in 2D and 3D Cell Culture

Sample	IC_{50} (μM) in 2D Cell Culture	IC_{50} (μM) in 3D Cell Culture	Fold Change
CCA-1.1	1.48	6.12	4.1
Doxorubicin	0.79	2.65	3.4

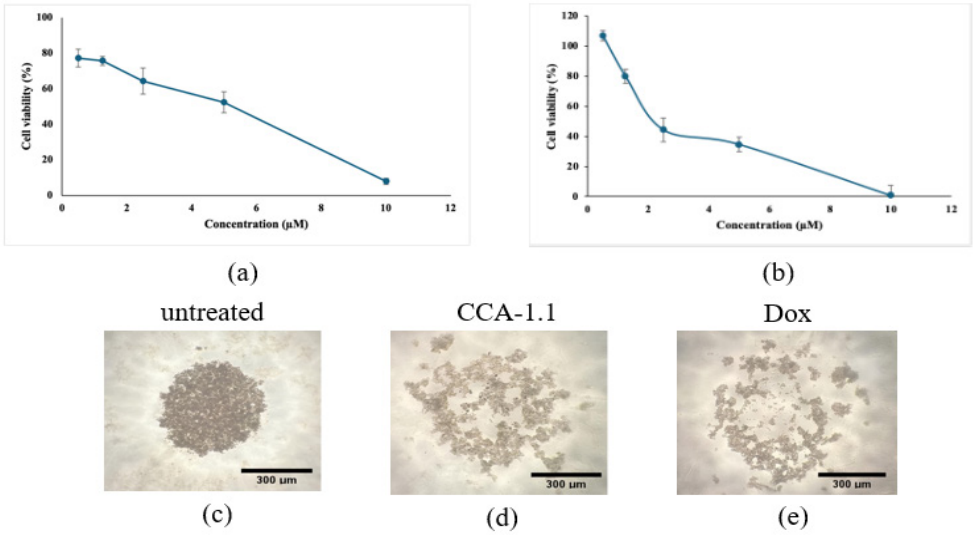

Figure 2. Cytotoxicity of CCA-1.1 and Doxorubicin in the MDA-MB-231 Agarose-based 3D Culture. The agarose-based 3D spheroid of MDA-MB-231 was prepared as detailed in the Methods. The cytotoxicity of (a) CCA-1.1 and (b) doxorubicin was assessed using CCK-8. Data represent mean ± SD from three independent experiments. The cell spheroid morphology of (c) the untreated group, (d) the CCA-1.1-treated group, and (e) the doxorubicin-treated group under an inverted microscope (total magnification 100×).

Doxorubicin remained the most potent (IC_{50} = 2.65 ± 0.30 μM), whereas CCA-1.1 required 6.12 ± 0.27 μM, respectively, to reach 50% inhibition. Bright-field imaging confirmed a concentration-dependent decrease in spheroid integrity and an increase in central translucency (Figure 2). When expressed as fold-change (3D/2D), drug tolerance increased 3.4-fold for doxorubicin and 4.1-fold for CCA-1.1, as shown in Table 2.

Spheroid-forming Assay

CCA-1.1 was further assessed for its effect on spheroid-forming capacity in MDA-MB-231 3D cultures. Untreated cells formed 8.3±0.6 spheroids per 50,000 cells, whereas CCA-1.1 at its 3D IC_{50} reduced spheroid number to 5.0±0.9 (≈40% inhibition vs. control). Doxorubicin almost completely abrogated spheroid formation, leaving only 0.3±0.2 spheroids (≈96% inhibition). Statistical analysis confirmed significant differences between control and CCA-1.1, as well as between CCA-1.1 and doxorubicin ($p<0.01$–0.001). These findings indicate that CCA-1.1 markedly suppresses spheroid-forming potential, although doxorubicin remains more potent in this agarose-based 3D spheroid model (Figure 3).

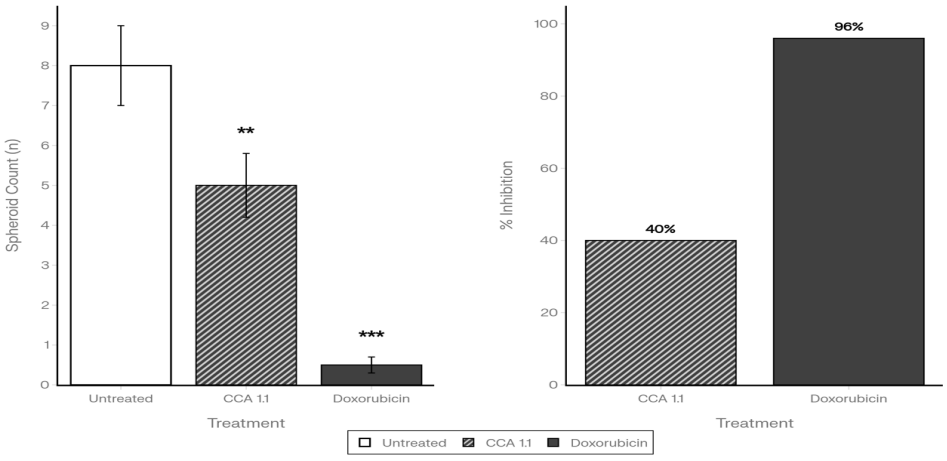

Figure 3. CCA-1.1 Effect on Spheroid Formation of MDA-MB-231 Triple-Negative Breast Cancer Cells. (a) Absolute spheroid count in untreated, CCA-1.1 (IC_{50}), and doxorubicin (IC_{50}) -treated cultures after 7 days (Data represent mean ± SE from three biological replicates). **$p<0.01$; ***$p<0.001$ vs. control. (b) Percentage inhibition of spheroid formation.

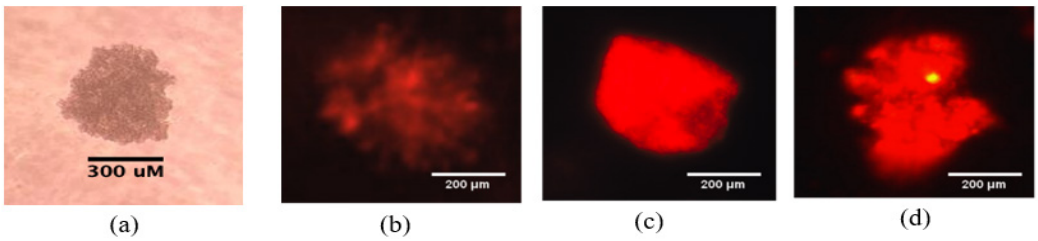

Figure 4. Evaluation of the MDA-MB-231 Cell Spheroid Response to CCA-1.1 using PI staining. (a) Phase contrast image of an untreated cell spheroid; (b) Propidium iodide staining of untreated cell spheroids; (c) CCA-1.1-treated, (d) doxorubicin (Dox)-treated.

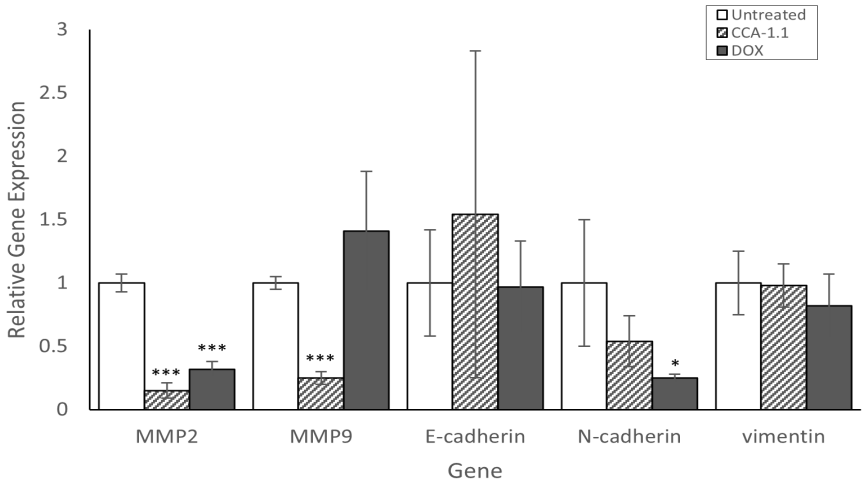

Figure 5. Relative mRNA Expression of Metastasis-Related and EMT Marker genes. Evaluation of the expression level of MMP2, MMP9, E-cadherin, N-cadherin, and vimentin in MDA-MB-231 3D spheroids was performed using qRT-PCR. The spheroids were treated with CCA-1.1 or doxorubicin compared to the untreated ones. Data represent fold change ± SE (n=3 biological replicates); statistical significance versus untreated is indicated as *p<0.05, ***p<0.001.

Spheroid Response Evaluation using PI staining

PI-positive fluorescence was minimal and diffuse in untreated spheroids, indicating low basal cell death, whereas doxorubicin markedly increased PI signal and disrupted spheroid architecture, consistent with extensive loss of viability. Moreover, CCA-1.1 produced a compact spheroid with intense PI fluorescence throughout, suggesting an induction of cell death while maintaining overall spheroid integrity (Figure 4).

Expression level of metastasis & EMT marker genes

Gene expression analysis of metastasis-related genes from the spheroid revealed that CCA-1.1 produced a strong inhibitory effect on *MMP2* and *MMP9* expression (Figure 5). *MMP2* levels decreased to 0.15±0.06 (p=0.0001) and *MMP9* to 0.25±0.05 (p<0.0001) relative to control, indicating a significant suppression of extracellular matrix–degrading capacity. Doxorubicin also significantly reduced *MMP2* expression (0.32±0.06; p=0.0002) but tended to increase *MMP9* (1.41±0.47; p=0.2068), suggesting a less consistent impact on metastatic potential (Figure 5). Furthermore, examination of EMT markers at the transcription level showed that CCA-1.1 increased *E-cadherin*, with a 1.5-fold increase compared to control (1.54±1.29; p=0.379). However, this was not significant. In addition, doxorubicin also did not significantly change *E-cadherin* levels (0.97±0.36; p=0.7721). Both treatments decreased *N-cadherin* expression; doxorubicin caused a statistically significant reduction (0.25±0.03; p=0.0463), whereas the decrease from CCA-1.1 was 0.56±0.20 (p=0.1747). *Vimentin* expression remained near baseline in all groups, with fold changes around 1.0, indicating that CCA-1.1 mainly influences cadherin switching rather than intermediate filament expression. Overall, these results indicate that CCA-1.1 has an anti-metastatic activity by significantly downregulating key metalloproteinases and enhancing epithelial characteristics. However, we did not conduct in vitro migration and invasion assays to clarify this finding.

Discussion

Our current research aims to develop a stable 3D culture system using agarose as the matrix. We grew the triple-negative breast cancer cell line MDA-MB-231 in agarose matrix to evaluate the potency of the curcumin analog, CCA-1.1, as a chemotherapeutic candidate in agarose-based 3D spheroid. Spheroids formed compact, uniformly spherical colonies by 72 hours. They maintained morphological integrity for at least 96 hours without spontaneous disassembly or the development of a necrotic core, suggesting that this platform sufficiently recapitulates the essential architectural characteristics of solid tumours amenable to intermediate-term drug

challenge [19]. Consistent spheroid size and no structural deterioration during treatment suggest that any observed alterations in cell viability and morphology are likely indicative of accurate cytotoxic responses to test compounds, rather than culture-related false positives/negatives [14]. The agarose matrix in 3D culture presented several advantages: 1) it allows for reproducible spheroid sizes and morphologies, and 2) it is easy to prepare without the use of costly scaffolds and is further compatible with well-known viability assays such as CCK-8 [20]. Real-time tracking of spheroid size and volume enabled simultaneous analysis of morphologic alterations and viability data, thereby enhancing the robustness of cytotoxicity profiling.

This work provides further evidence that 3D microsystems composed of agarose more closely reflect realistic physiological conditions for tumor microenvironment modeling than traditional 2D cultures on a flat surface. The in vitro 3D spheroids from MDA-MB-231 displayed drug-resistance features that more closely resemble those of an in vivo counterpart, as we found much higher IC_{50} values for all compounds compared to those in monolayer cells. CCA-1.1 was 4.1-fold for IC_{50} in 3D-spheroids and was ~3.4-fold higher for doxorubicin. These results are consistent with many previous reports that 3D spheroids more accurately mimic the physiological drug resistance observed in vivo, including restricted drug penetration, oxygen and nutrient gradients, and increased cell–cell and cell–matrix communication [21-23]. The relative fold-changes for doxorubicin and CCA-1.1 may be attributed to their differences in physical-chemical properties among these compounds. The IC_{50} of doxorubicin for 2D cultures and 3D spheroids aligns with previously reported values (0.58–1.0 μM for 2D and 2–3 μM for various 3D models) [21-22], validating our experimental procedure.

CCA-1.1 is not the only curcumin analog that has been investigated against the MDA-MB-231 cell line. Zhao et al. [24] reported that EF-24 induces the initiation of autophagy and apoptosis in MDA-MB-231 cells, which is mediated by the ROS pathway. Another recent study from Ros et al. [25] shows that TL3 and TL4, synthetic curcumin analogs, have a lower IC_{50} value against MDA-MB-231 compared to curcumin, with IC_{50} values of 0.93 and 0.86 μM, respectively. Moreover, these curcumin analogs also displayed a lower mammosphere formation index (MFI) on the breast cancer stem cell (BCSC) population of MDA-MB-231 compared to curcumin. Our group also studied another curcumin analog, namely PGV-1, which exhibits irreversible antiproliferative effects in MDA-MB-231 (TNBC) and HCC1954 (HER2-overexpressing) cells with IC_{50} of 0.9 and 0.4 μM, respectively. CCA-1.1 in the current study has an IC_{50} of 1.48 μM, a similar value to a previous report by Novitasari et al. [11]. Although CCA-1.1 is less cytotoxic to MDA-MB-231 than other curcumin analogs, it shows a higher selectivity index compared to PGV-1. The selectivity index (SI) for CCA-1.1 and PGV-1 has been reported by Novitasari et al. [8], with SI values of 4.3 and 3.8, respectively, against TNBC 4T1 cells and fibroblast 3T3 cells. Our data of CCA-1.1 in agarose-based 3D spheroids improves the physiological relevance of elucidating its potency as a chemotherapeutic candidate.

Our investigation of spheroid-forming capacity indicated that CCA-1.1 reduced spheroid formation to a greater extent than the untreated control. The staining of propidium showed low basal PI fluorescence in the untreated spheroids, whereas both CCA-1.1 and doxorubicin resulted in substantial elevations of PI signal, indicating an induction of cell death in the 3D model. However, the spatial distribution in PI fluorescence images was altered considerably. Doxorubicin-treated spheroids displayed extensive PI staining, coupled with disruption of spheroid architecture and loss of structural integrity, indicative of an acute cytolytic/necrotic cell death program. In contrast, CCA-1.1-treated spheroids retained an overall compact morphology and PI signal throughout, in line with a programmed form of cell death driven by localised phenomena, without loss of overall spheroid structure. This dissimilar morphological change is likely due to distinct cell death mechanisms triggered by doxorubicin and CCA-1.1. Doxorubicin exerts cytotoxicity primarily by intercalating DNA, causing DNA damage and inhibiting topoisomerase II, producing rapid, membrane-permeabilizing cell death [26, 27]. On the other hand, CCA-1.1, with several mechanisms, including the production of reactive oxygen species (ROS), regulation of NF-κB signaling pathways, and cell cycle blockage due to mitotic dysfunction, might involve slower apoptosis or autophagy [8, 11-12, 28]. These mechanisms can give a chance of drug penetration and cell death maintenance while preserving the 3D structure.

Our study showed that CCA-1.1 inhibited *MMP2* and *MMP9* expression significantly, whereas doxorubicin only decreased *MMP2* but not *MMP9*. Previously, it was reported that CCA-1.1 and PGV-1 inhibit WiDr colon cancer cell migration and decrease *MMP9* levels, whereas doxorubicin induces both [9]. The suppression of *MMP2* and *MMP9* is important for the regulation of cancer metastasis as they mediate the cleavage of *E-cadherin* and convert it to soluble *E-cadherin*, leading to epithelial-mesenchymal transition (EMT) [29]. Quantitative analysis of the expression of EMT-related genes showed that CCA-1.1 elevated the expression of *E-cadherin* (despite the non-significant difference with untreated cells), a key marker of epithelial phenotype and cell adhesion. The upregulation of *E-cadherin* expression is critical for regaining epithelial properties under the conditions of EMT [30]. Additionally, the CCA-1.1 treatment did not affect *N-cadherin* levels and *Vimentin*, which may reflect a partial anti-EMT of CCA-1.1 on the TNBC. The inhibition of MMP and increased expression of *E-cadherin* by CCA-1.1 indicate its potential to prevent cancer cell invasion and metastatic spread and to restrain tumor cell migration. However, in the current study, we didn't perform further investigation on cell migration and invasion. Therefore, more studies are still needed to clarify this point.

The use of agarose-based spheroid models is not ideal for investigating cell migration and invasion in 3D culture because agarose is a non-adherent hydrogel; therefore, it does not provide cell-matrix adhesion comparable to that of collagen or laminin, which facilitates cell motility and

cell-matrix interaction [31]. The lack of mimicking the extracellular matrix limits the use of agarose for studying migration. Our findings can be further examined using an extracellular matrix-like gel, such as collagen, to better mimic the tumor environment.

Although these positive results are encouraging, this study is limited by the use of a single cancer cell line and the absence of mechanistic assays, including apoptosis, cell migration, and invasion. Informative studies using pairs of TNBC lines, patient-derived organoids, and co-culture with stromal/immune cells will give a comprehensive view of drug responses and function under physiologically relevant conditions. Furthermore, integrating CCA-1.1 with combinatorial regimens and traditional chemotherapies may exploit synergistic effects to overcome established mechanisms of resistance.

In conclusion, our study using a 3D agarose-based spheroid culture confirms CCA-1.1 cytotoxicity against MDA-MB-231. It shows that CCA-1.1 inhibits spheroid formation, reduces the expression level of matrix metalloproteinase, and tends to prevent cancer cells from transitioning to a mesenchymal phenotype. These data demonstrate the utility of agarose-based 3D spheroids for evaluating drug responses in TNBC cells, and support the development of CCA-1.1 as a chemotherapeutic candidate for TNBC.

Author Contribution Statement

RIJ, SMH, and MI were involved in concepting and planning the research. IRS and MI performed the data acquisition/collection. RIJ and IRS analyzed the experimental data. RIJ, IRS, and MI drafted the manuscript and designed the Figures. SMH, CO, and IMJ contributed to data analysis and interpretation. All authors took part in giving a critical revision of the manuscript.

Acknowledgements

Funding Statement

We appreciate the research funding from the Directorate of Research and Community Service, the Directorate General of Research and Development, Ministry of Higher Education, Science, and Technology, Indonesia, under the 2025 Regular Fundamental Research scheme (grant number 2417/UN1/DITLIT/Dit-Lit/PT.01.03/2025).

Approval

This study was part of the dissertation of Ika Rahmawati Sutejo as a student in the Doctoral Program of Biotechnology, School of Postgraduate, Universitas Gadjah Mada.

Ethical Declaration

This study was approved by the Ethics Committee of Medical and Health Research Ethics Committee (MHREC), Faculty of Medicine, Public Health and Nursing, Universitas Gadjah Mada - Dr. Sardjito General Hospital, Indonesia. The approval reference number is KE/FK/1238/EC/2025.

Conflict of Interest

The authors declare that there is no conflict of interest

References

1. Vyas A, Dwivedi S, Koka SS, Darwhekar GN. Triple negative breast cancer: molecular subtypes, therapeutic challenges, and emerging strategies- a systematic review. Premier J Sci. 2025;1(1):e100101. https://doi.org/10.70389/pjs.100101 .
2. Xiong N, Wu H, Yu Z. Advancements and challenges in triple-negative breast cancer: A comprehensive review of therapeutic and diagnostic strategies. Front Oncol. 2024;14:1405491. https://doi.org/10.3389/fonc.2024.1405491
3. Zagami P, Carey LA. Triple negative breast cancer: Pitfalls and progress. NPJ Breast Cancer. 2022;8(1):95. https://doi.org/10.1038/s41523-022-00468-0
4. Huang M, O'Shaughnessy J, Zhao J, Haiderali A, Cortés J, Ramsey SD, et al. Economic and humanistic burden of triple-negative breast cancer: a systematic literature review. Pharmacoeconomics. 2022;40(6):519-58. https://doi.org/10.1007/s40273-021-01121-7.
5. Biju TS, Priya VV, Francis AP. Role of three-dimensional cell culture in therapeutics and diagnostics: an updated review. Drug Deliv Transl Res. 2023;13(9):2239-53. https://doi.org/10.1007/s13346-023-01327-6.
6. Varshini MS, Krishnamurthy PT, Reddy RA, Wadhwani A, Chandrashekar VM. Insights into the emerging therapeutic targets of triple-negative breast cancer. Curr Cancer Drug Targets. 2024;24(1):e0115680096280750. https://doi.org/10.2174/0115680096280750240123054936.
7. Mardaneh P, Lavian S, Bagherniya M, Roufogalis BD, Sahebkar A. Synthetic curcumin analogs in the treatment of cancer: a literature review. Curr Med Chem. 2024;32(17):3366-88. https://doi.org/10.2174/0109298673256932231123151626.
8. Novitasari D, Jenie RI, Utomo RY, Kato J, Meiyanto E. CCA 1.1, a novel curcumin analog, exerts cytotoxic anti migratory activity toward triple negative and HER2 enriched breast cancer cells. Asian Pac J Cancer Prev. 2021;22(6):1827-36. https://doi.org/10.31557/APJCP.2021.22.6.1827.
9. Wulandari F, Ikawati M, Kirihata M, Kato JY, Meiyanto E. Curcumin Analogs, PGV-1 and CCA-1.1 Exhibit Anti-Migratory Effects and Suppress *MMP9* Expression on WiDr Cells. Indones Biomed J. 2021;13(3):271-80. doi:10.18585/inabj.v13i3.1583.
10. Utomo RY, Wulandari F, Novitasari D, Lestari B, Susidarti RA, Jenie RI, et al. Preparation and cytotoxic evaluation of pgv-1 derivative, cca-1.1, as a new curcumin analog with improved-physicochemical and pharmacological properties. Adv Pharm Bull. 2022;12(3):603-12. https://doi.org/10.34172/apb.2022.063.
11. Novitasari D, Jenie RI, Kato JY, Meiyanto E. Chemoprevention curcumin analog 1.1 promotes metaphase arrest and enhances intracellular reactive oxygen species levels on tnbc mda-mb-231 and her2-positive hcc1954 cells. Res Pharm Sci. 2023;18(4):358-70. https://doi.org/10.4103/1735-5362.378083
12. Moordiani M, Novitasari D, Susidarti RA, Ikawati M, Kato J, Meiyanto E. Curcumin analogs PGV 1 and CCA 1.1 induce cell cycle arrest in human hepatocellular carcinoma cells with overexpressed MYCN. Indones Biomed J. 2023;15(3):270-9. https://doi.org/10.18585/inabj.v15i2.2147.
13. Esposito A, Ferraresi A, Vallino L, Garavaglia B, Dhanasekaran DN, Isidoro C. Three-dimensional in vitro cell cultures as a feasible and promising alternative to two-dimensional and animal models in cancer research. Int J Biol Sci. 2024;20(13):5293-311. https://doi.org/10.7150/ijbs.96469.

14. Tang J, Lebedeva Y, Dey S, Chen Y, Zhang S, Hoey C, et al. Advances in 3D cell culture for drug screening and toxicology evaluation. Front Bioeng Biotechnol. 2023;11:1266506. https://doi.org/10.3389/fbioe.2023.1266506.
15. Imamura Y, Mukohara T, Shimono Y, Funakoshi Y, Chayahara N, Toyoda M, et al. Comparison of 2D- and 3D-culture models as drug-testing platforms in breast cancer. Oncol Rep. 2015;33(4):1837-43. https://doi.org/10.3892/or.2015.3767.
16. Huang Z, Yu P, Tang J. Characterization of triple-negative breast cancer mda-mb-231 cell spheroid model. Onco Targets Ther. 2020;13:5395-405. https://doi.org/10.2147/ott.S249756
17. Debruyne AC, Okkelman IA, Heymans N, Pinheiro C, Hendrix A, Nobis M, et al. Live microscopy of multicellular spheroids with the multimodal near-infrared nanoparticles reveals differences in oxygenation gradients. ACS Nano. 2024;18(19):12168-86. https://doi.org/10.1021/acsnano.3c12539.
18. Brüningk SC, Rivens I, Box C, Oelfke U, Ter Haar G. 3d tumour spheroids for the prediction of the effects of radiation and hyperthermia treatments. Sci Rep. 2020;10(1):1653. https://doi.org/10.1038/s41598-020-58569-4.
19. Nag M, Ströbel S, Hutter S, Issa T, Ligeon L, Goedecke N, et al. Abstract 1220: Cryopreserved 3D human tumor spheroid platform in 96 well format for robust and scalable discovery and screening. Cancer Res. 2025;85(8 Suppl 1):1220. https://doi.org/10.1158/1538-7445.AM2025-1220.
20. Krishnan MA, Yadav K, Chelvam V. Agarose micro-well platform for rapid generation of homogenous 3d tumor spheroids. Curr Protoc. 2021;1(7):e199. https://doi.org/10.1002/cpz1.199.
21. Berrouet C, Dorilas N, Rejniak KA, Tuncer N. Comparison of drug inhibitory effects (IC_{50}) in monolayer and spheroid cultures. Bull Math Biol. 2020;82(6):68. https://doi.org/10.1007/s11538-020-00746-7.
22. Abbas ZN, Al-Saffar AZ, Jasim SM, Sulaiman GM. Comparative analysis between 2d and 3d colorectal cancer culture models for insights into cellular morphological and transcriptomic variations. Sci Rep. 2023;13(1):18380. https://doi.org/10.1038/s41598-023-45144-w
23. Passos CL, Polinati RM, Ferreira C, Dos Santos NA, Lima DG, da Silva JL, Fialho E. Curcumin and melphalan cotreatment induces cell cycle arrest and apoptosis in MDA-MB-231 breast cancer cells. Sci Rep. 2023;13(1):13446. https://doi.org/10.1038/s41598-023-40535-5
24. Zhao YY, Li J, Wang HQ, Zheng HB, Ma SW, Zhou GZ. Activation of autophagy promotes the inhibitory effect of curcumin analog ef-24 against mda-mb-231 cancer cells. J Biochem Mol Toxicol. 2024;38(2):e23642. https://doi.org/10.1002/jbt.23642
25. Ros M, Riesco-Llach G, Polonio-Alcalá E, Morla-Barcelo PM, Ruiz-Martínez S, Feliu L, et al. Inhibition of Cancer Stem-like Cells by Curcumin and Other Polyphenol Derivatives in MDA-MB-231 TNBC Cells. Int J Mol Sci. 2024;25(13):7446. https://doi.org/10.3390/ijms25137446.
26. Beretta GL, Zunino F. Molecular mechanisms of anthracycline activity. Top Curr Chem. 2008;283:1-19. https://doi.org/10.1007/128_2007_3.
27. Pilco-Ferreto N, Calaf GM. Influence of doxorubicin on apoptosis and oxidative stress in breast cancer cell lines. Int J Oncol. 2016;49(2):753-62. https://doi.org/10.3892/ijo.2016.3558.
28. Utomo RY, Hapsari NP, Nugraheni N, Lestari B, Hanifa M, Linda Laksmiani NP, et al. CCA-1.1 Destabilizes MYC proteins to induce irreversible anti-proliferative effects in hepatocellular carcinoma. Med Oncol. 2025;43(1):34. https://doi.org/10.1007/s12032-025-03135-z.
29. Tune BXJ, Sim MS, Poh CL, Guad RM, Woon CK, Hazarika I, et al. Matrix Metalloproteinases in Chemoresistance: Regulatory Roles, Molecular Interactions, and Potential Inhibitors. J Oncol. 2022;2022:3249766. https://doi.org/10.1155/2022/3249766.
30. Kang Y, Massagué J. Epithelial-mesenchymal transitions: Twist in development and metastasis. Cell. 2004;118(3):277-9. https://doi.org/10.1016/j.cell.2004.07.011.
31. Chong LH, Yip AK, Farm HJ, Mahmoud LN, Zeng Y, Chiam KH. The role of cell-matrix adhesion and cell migration in breast tumor growth and progression. Front Cell Dev Biol. 2024;12:1339251. https://doi.org/10.3389/fcell.2024.1339251.